Iteratively re-weighted least squares inversion for the estimation of density from well logs: part two

A. Nassir Saeed, Laurence R. Lines, and Gary F. Margrave

ABSTRACT

Incorporating of constrains in data-misfit domain is tested in this part of study. The inverted density model has resolved different lithology layers, and successfully delineated gas-bearing sand reservoir of the Blackfoot. The additional information incorporated into the weighted matrices used by inverse algorithm has enhanced the interpretation of inverted density log significantly; in particular, the sand base-line as well as separation of sand and carbonate regions. Joint-inversion of Vp and Vs logs to predict density log has shown some improvements of final shape of density log.

INTRODUCTION

In part one of this study, the theory of IRLS along with building of L-curve function to obtain an optimum trade-off parameter that led to smooth convergence towards final model were given. Although, constrains imposed into model space domain showed fast and stable convergence, yet the RMS error did not show a Gaussian curve-shape (i.e., error did not decrease as we converge towards final model solution).

In this paper, we will investigate the produced model and *RMS* error curve by imposing constrains in the data-misfit. The stability of proposed inverse algorithm will also be tested by using noisy log. Furthermore, the accuracy of the final density model will be investigated further by using joint-inversion of multi logs.

IRLS INVERSION OF DENSITY LOG

Recall equation (15) from part one. The re-weighted least squares inverse equation is given by

$$(G^T W_d^T R_d W_d G + \lambda W_m^T R_m W_m) m = G^T W_d^T R_d W_d d \qquad (1)$$

Note that the model regularization operator, $\mathbf{W_m}$, was set to be first-order difference operator during this part of study. In the following subsections, the use of different constrains in data-misfit space is explained.

The weight matrix w_d

Several methods to estimate the weighted matrix $\mathbf{W_d}$ have been tested and incorporated in the data misfit domain. These weight matrices have size of M x M, where zeros take up much spaces of the matrices sizes. One can utilize the sparse matrix technique (Varga, 1962) where only non-zero values with their indices are saved in disk memory. In the following subsections, explanations for each of weight method used are given.

Standard deviation of measured and residual

In geophysical inversion, it is assumed that the model parameter errors are independent and normally distributed (Aster et. al., 2005). Typically, W_d contain information about standard deviation of measurement error. For the fist iteration, W_d in equation (1) was set to be identity matrix, and for subsequent iterations, the standard deviation is calculated by

$$\sigma = \sqrt{\frac{1}{m-n}\sum_{i=1}^{m} r_i^2} \tag{2}$$

Note that in equation (1), the weighted matrix, $\boldsymbol{W_d}$, is scaled by the measured field density data, $\boldsymbol{d^{obs}}$, in order to test the stability of the algorithm. Figure (1) shows the inverted section of density log, while figure (2) is a display of RMS plotted for all iterations.

Robustness normalized by Std. deviation

The fractional $\ell_1 - \ell_2$ norm scaled by standard deviation (Rücker and Günther, 2006) is also tested in this study. The weighted function is written in explosive form as,

$$\kappa = \left(\frac{|e\,1|^1}{\|e\|_1^1} \Big/ \frac{|e\,1|^2}{\|e\|_2^2} \right) \Big/ \sigma \tag{3}$$

Figure (3) show the inverted density log, while figure (4) is associated *RMS* error during inversion. Note that the final model converged towards the final model within few numbers of iterations compared to previous constraint methods used.

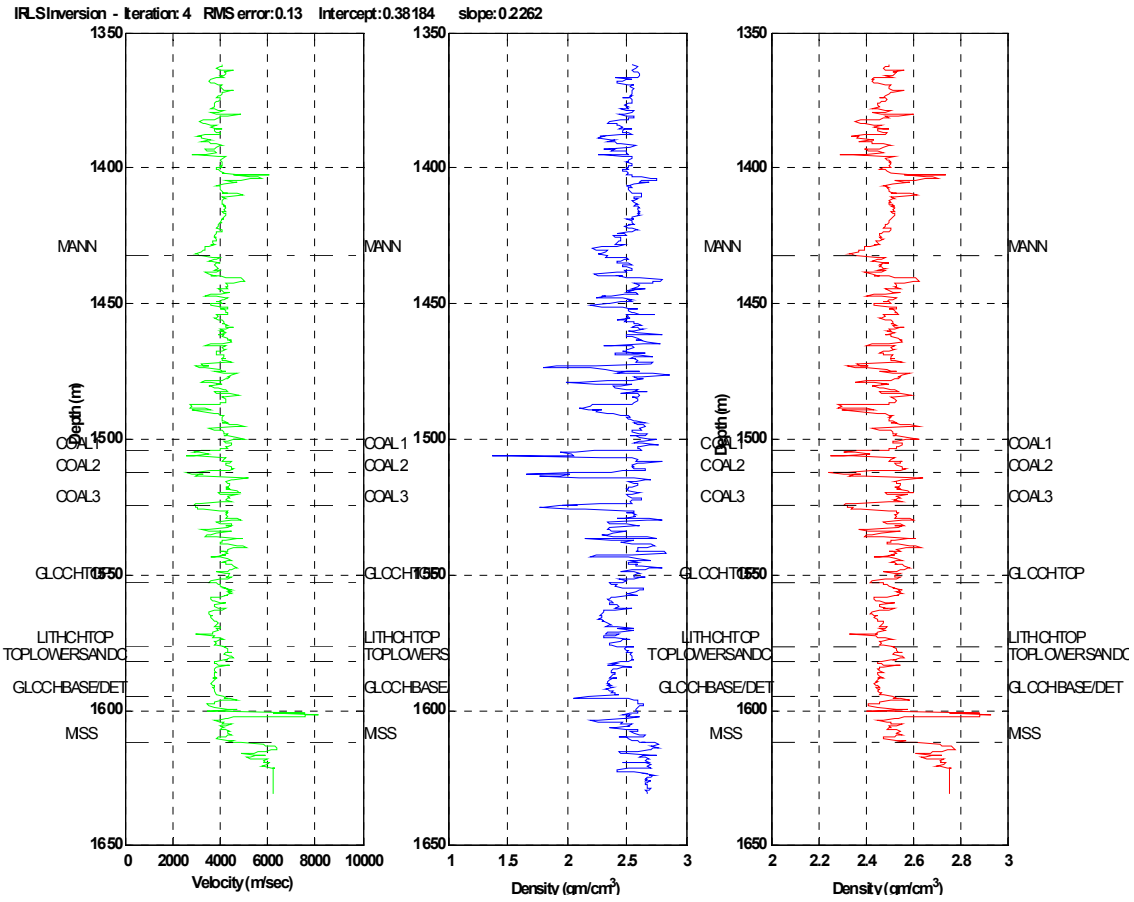

FIG.1.Well 08-08: IRLS inversion of density log. $W_d = \sigma$

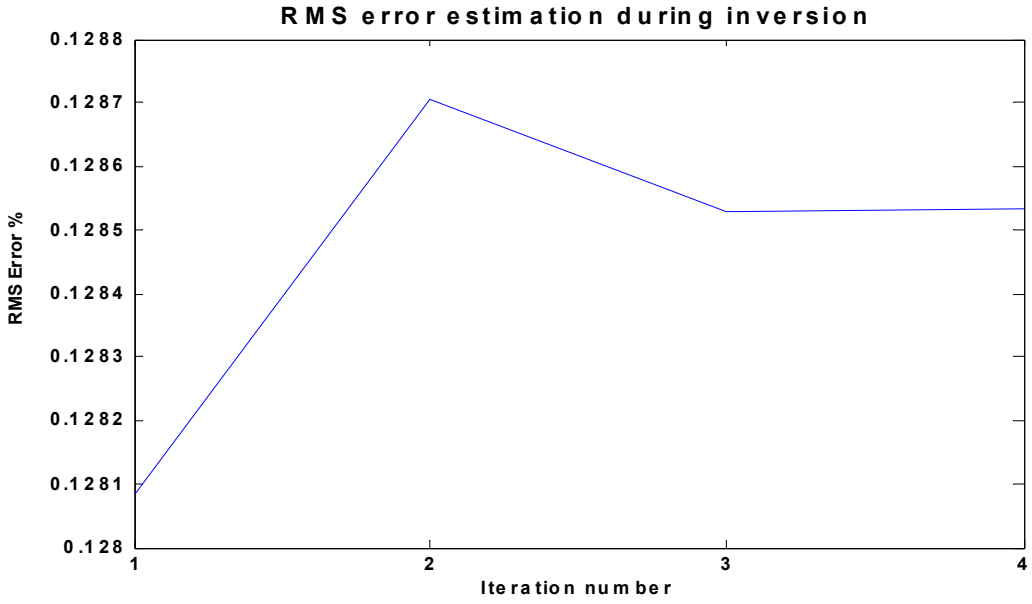

FIG.2.Well 08-08: *RMS* error during IRLS inversion of density log. $W_d = \sigma$

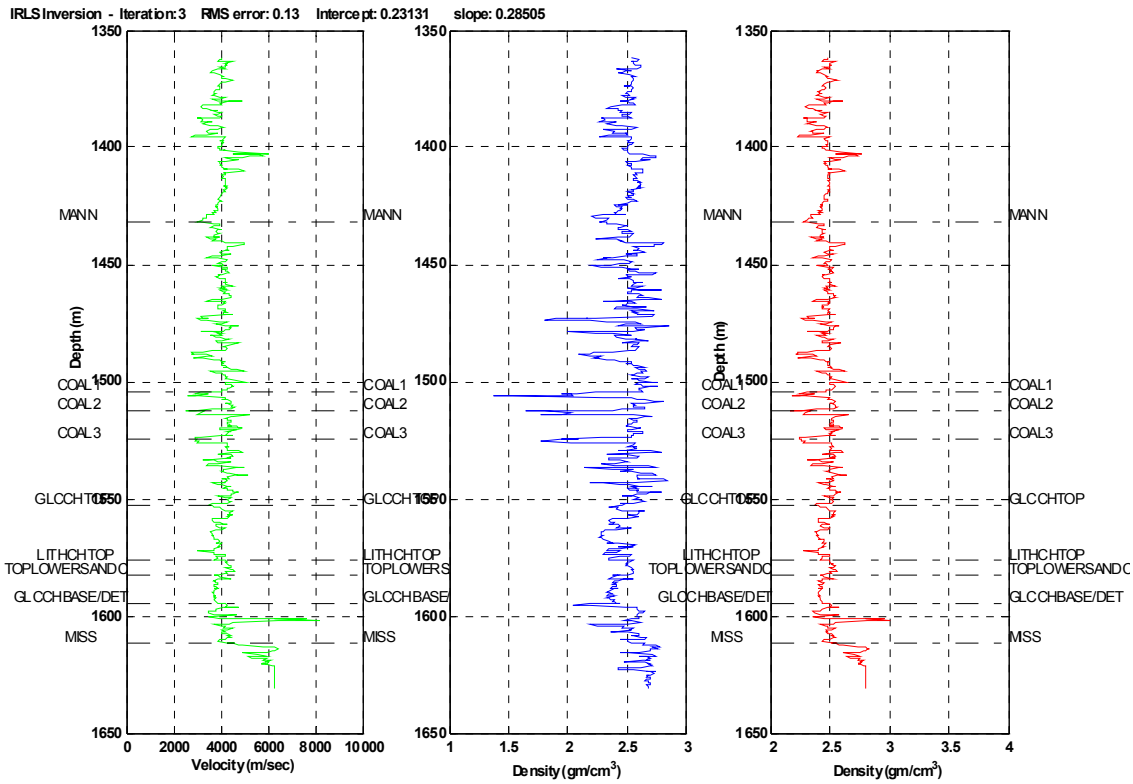

FIG.3. Well 08-08: IRLS inversion of density log using fractional $\ell_1 - \ell_2$ norms scaled by standard deviation.

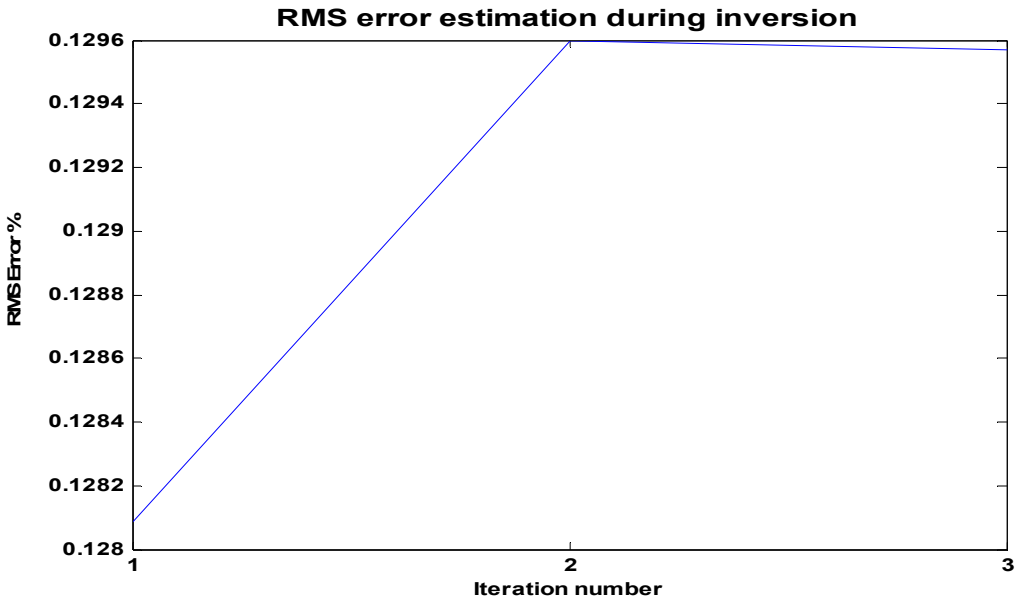

FIG.4. Well 08-08: RMS error during IRLS inversion of density log using fractional $\ell_1 - \ell_2$ norms scaled by standard deviation.

Hybrid ℓ_1/ℓ_2 norms

The hybrid ℓ_1/ℓ_2 norms (Bube and Langan, 1997) method is also tested in this study. The norms were scaled by modified Darche(1989) tuning constant τ. The modified *Darche*, (1989) threshold τ, that can be used as tuning constant, is written as,

$$\tau = \frac{\max|r|}{100} \tag{4}$$

where r is residual.

The hybrid ℓ_1/ℓ_2 norm is then written as

$$W_{ii} = \left[1 + (r_i/\tau)^2\right]^{-0.25} \tag{5}$$

The inverted density log is given in figure (5), while the RMS error in figure (6) converges to pre-set tolerant limit.

Huber and Tukey's constraints

The maximum likelihood estimator, often referred as M-estimator, has been widely used in linear regression problems (Hong and Chen, 2005) to reduce the influence of outliers. The M-estimator is defined as the solution of the minimization cost function, which can be expressed as,

$$g(x) = \sum_{i=1}^{N} \rho \frac{(r_i(x))}{s} \tag{6}$$

Where ρ is an even, continuously differential function (Wolke and Schwetlick, 1998), *s* is a scaling factor of the residual r_i. The scaling parameter, *s,* used in this study is the median absolute deviation, MAD (Holland and Welsch, 1977). The most common M-estimators are the *Huber* estimator (Huber, 1981), and is written as

$$\rho_H(r) = \begin{cases} \frac{1}{2} r^2 & for\ |r| \le \xi \\ \xi|r| - \frac{1}{2}\xi^2 & for\ |r| > \xi \end{cases} \tag{7}$$

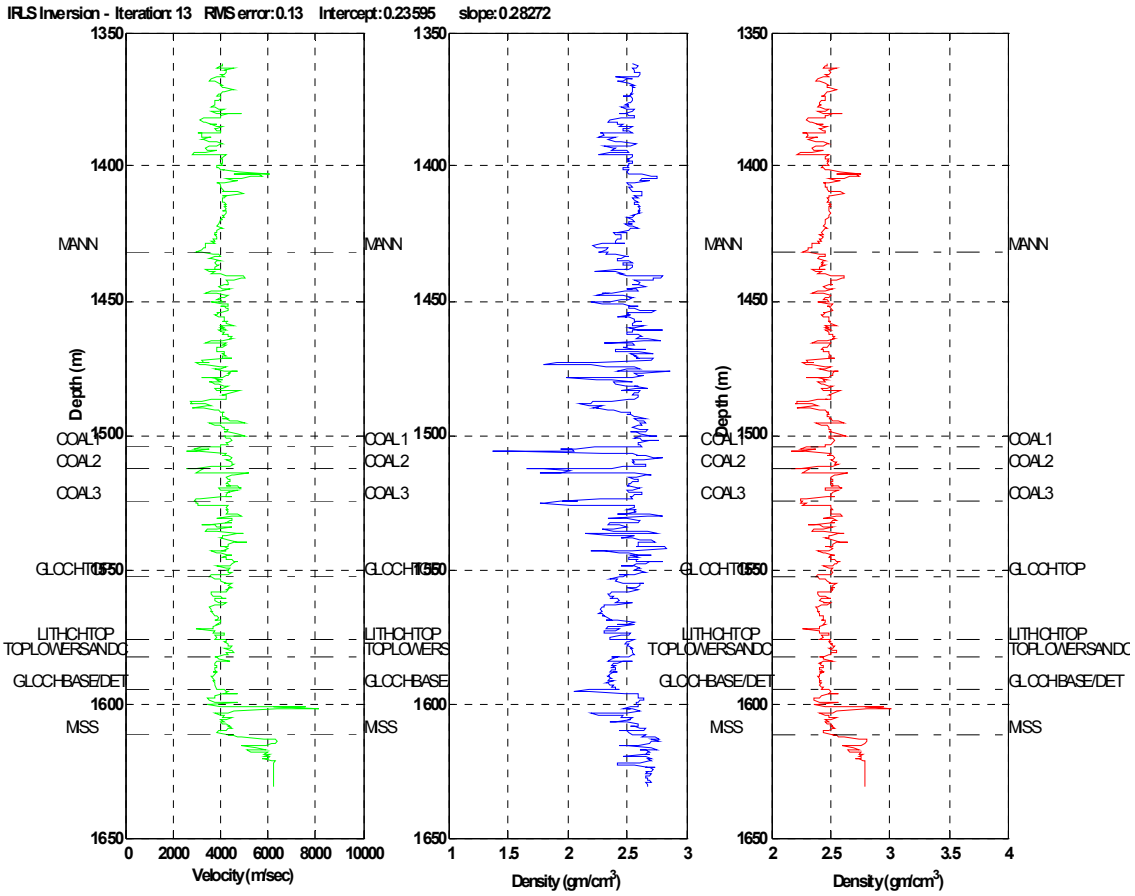

FIG.5. Well 08-08: IRLS inversion of density log using hybrid $\ell_1 - \ell_2$ norms.

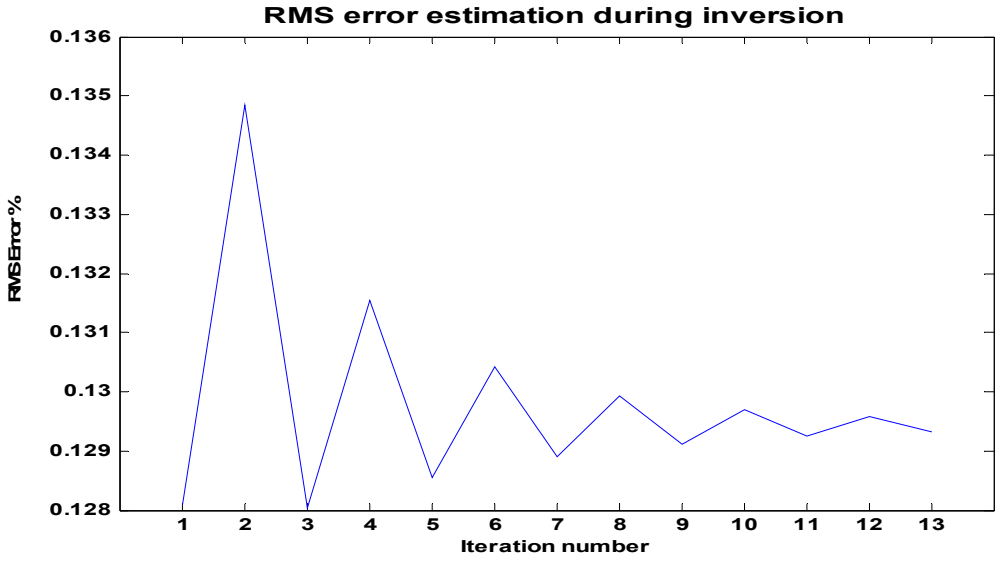

FIG.6. Well 08-08: RMS error during IRLS inversion of density log using hybrid ℓ_1 / ℓ_2 norms.

While the Tukey bi-square estimator (Tukey, 1960) is written as,

$$\rho_T(r) = \begin{cases} \frac{\xi^2}{6}\left\{1-\left[1-(\frac{r}{\xi})^2\right]^3\right\} & for\ |r| \le \xi \\ \frac{1}{6}\xi^2 & for\ |r| > \xi \end{cases} \tag{8}$$

where ξ is a tuning constant.

It is common to choose $\xi = 1.345\sigma$ for *Huber* estimator and $\xi = 4.685\sigma$ for *Tukey* bi-square (or bi-weight) estimator, since these values offer robustness against outliers, yet produce 95% efficiency when the error are normally distributed (Huber, 1981).

Denote *k* as iteration step, the weight function for Huber and Turkey can be explicitly written as

$$\omega_H^{(k)} = \begin{cases} 1 & for\ \ |r^{(k-1)}| \le \xi \\ \frac{\xi}{\left|r^{(k-1)}\right|} & for\ \ |r| > \xi \end{cases} \tag{9}$$

$$\omega_T^{(k)} = \begin{cases} \left[1-(\frac{r^{(k-1)}}{\xi})^2\right]^2 & for\ |r^{(k-1)}| \le \xi \\ 0 & for\ |r| > \xi \end{cases} \tag{10}$$

Because ω is a prior unknown, an iteratively reweighted least square (IRLS) inversion is required. Note that the tuning constant given earlier did not produce a converged solution for equation (1). Therefore a modification for the tuning constant is needed to stabilize the IRLS inverse algorithm. In this study, a modification of Huber's and Darche's estimated tuning constant is established. The new tuning constant for Huber and Tukey weight function are respectively written as,

$$\xi_H = 1.345\,\frac{\max|r|}{100} \tag{11}$$

$$\xi_T = 4.685 \frac{\max|r|}{100} \tag{12}$$

The new tuning constants in equations (11 and 12) are used, and have shown some improvement in terms of convergence and accuracy for resulting models. However, the scale parameter of the *median absolute deviation*,(MAD) has shown better convergence among other tuning constants in producing final inverted section (figure 7) using Huber weight function. The RMS error in figure (8) reaches minimum level.

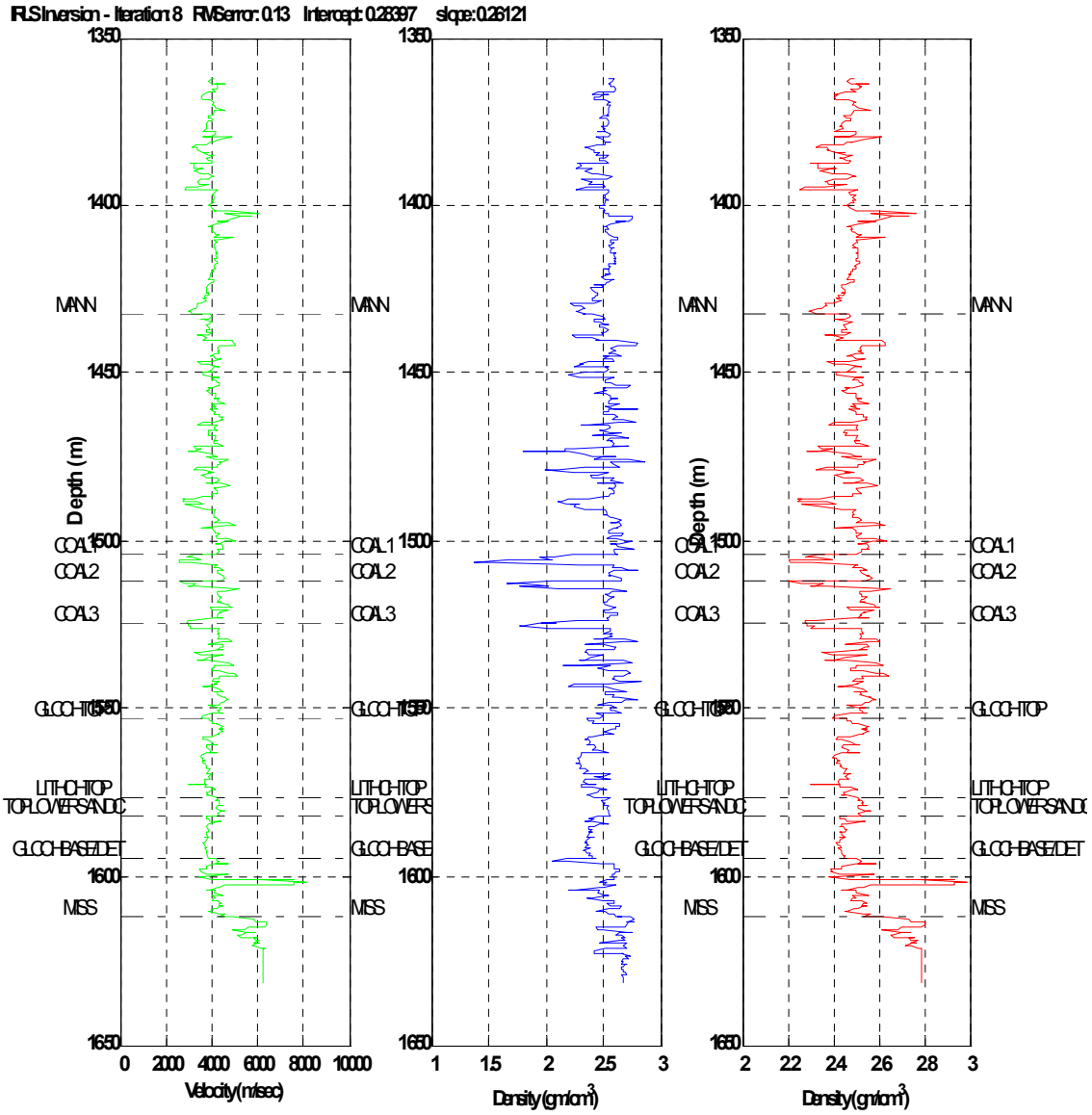

FIG.7. Well 08-08: IRLS inversion of density log using Huber weight function.

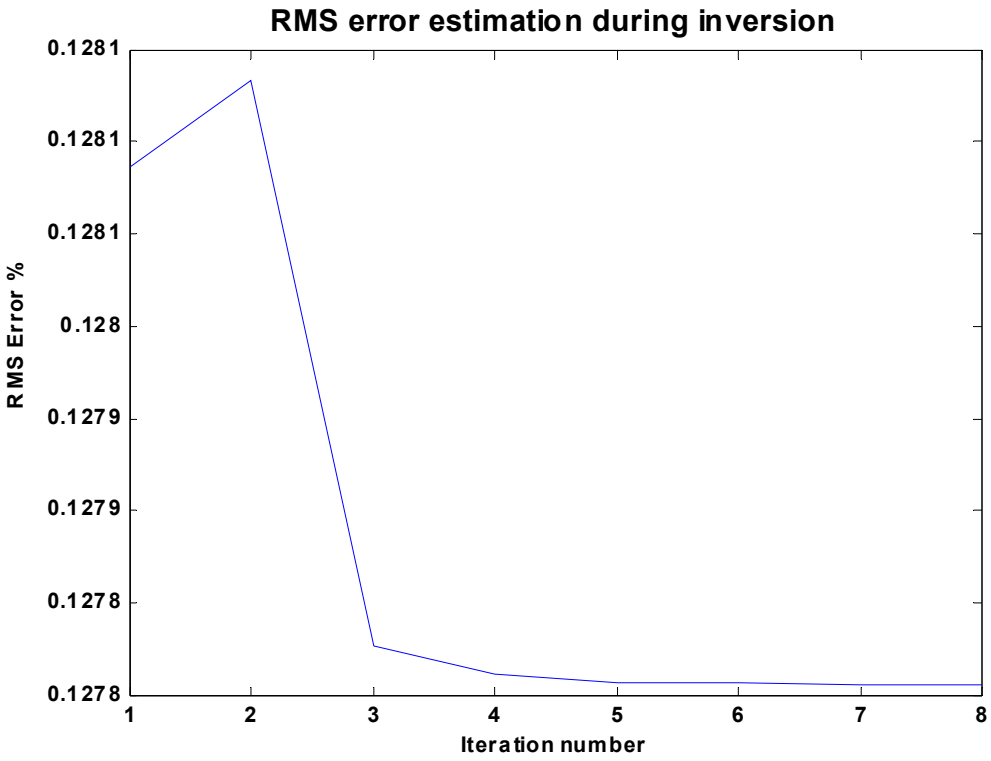

FIG.8. Well 08-08: RMS error during IRLS inversion using Huber weight function.

The inverted section in figure (9) by using bi-square Tukey weight function shows slight difference compared to the inverted section in figure (7) using the Huber weight function. However, the RMS error in figure (10) is slightly higher than of the Huber weight function (see figure, 8). Furthermore, the intercept and slope values estimated using Tukey weight function shows lowest intercept and higher slope values respectively compared to previous weight functions used in data and model domains.

The Annealing M-Estimator

The RMS error graphs in previous section have shown oscillations of error as program tried to converge to pre-set tolerance value. In order to stabilize convergence issue, *Li*, (1996) presented a modified robust M-estimator called annealing M-estimator, often referred as **AM**-Estimator. It gives a global solution, and is very stable and has good behavior in regards to percentage of outliers and noise variance.

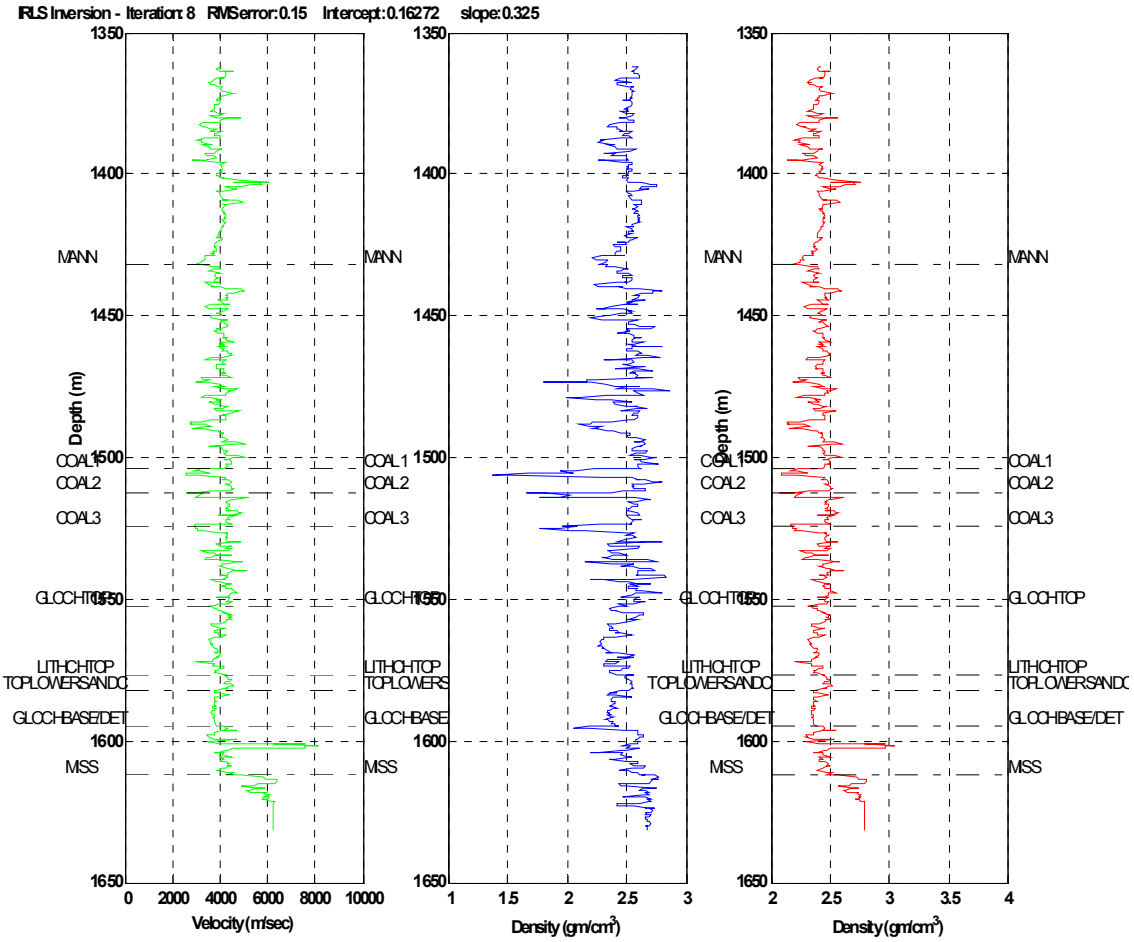

FIG.9. Well 08-08: IRLS inversion of density log using Tukey bi-square weight function.

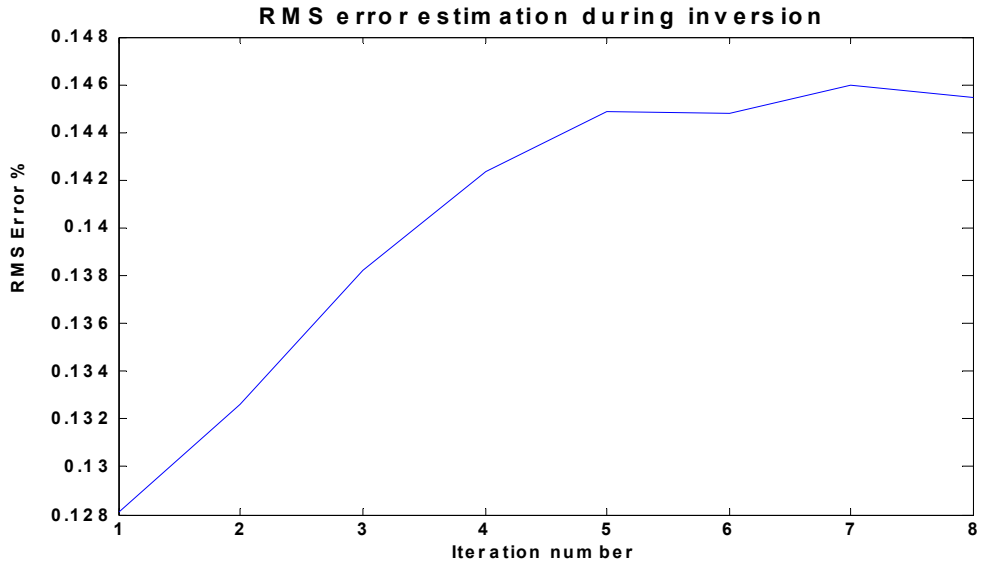

FIG.10. Well 08-08: RMS error during IRLS inversion using Tukey weight function.

The scale, *s*, in M-function is replaced by parameter γ in AM-estimator that is approaching 0^+ during the processing. The AM-estimator under γ is defined by

$$f_\gamma = \frac{\sum_i h_\gamma(\eta_i) r_i}{\sum_i h_\gamma(\eta_i)} \tag{13}$$

where $h_\gamma(\eta_i)$ is an adaptive interaction function parameterized by γ (Li, 1996).

The adaptive interaction function is given by

$$h_\gamma(\eta_i) = \frac{1}{1 + (\eta^2 / \gamma)} \tag{14}$$

Where h_γ acts as interaction weighting function and $\eta_i = r_i$.

In the inversion algorithm, the parameter γ was initially set equal to the Huber tuning constant, $\xi_i = 1.345\sigma$ and then minimized after 1st iteration by $\xi_{i+1} = \xi_i - \xi_i / 4$. Figure (11) shows the inversion model of density log, while figure (12) shows a good convergence where the RMS error reached a minimum magnitude after 4th iteration.

COMPARISONS OF RESULTS FROM MODEL AND DATA CONSTRAINS

The plot in figure (13) shows the measured density plotted versus predicted density (where weight was added to data-space) while the residual is color coded. Figure (14) shows same plot but for weight in model-space. Note that the residual in model-space is slightly higher than residual resulted from weight imposed to data-space.

However, both figures show that majority of point have small magnitude of residuals. Furthermore, these figures allow us examine points with high residual that are substantially having high error percentage. Hence, one can later either adjust or trim these outliers.

A successful inverse algorithm is achieved when its residual follows a Gaussian error distribution (Claerbout and Muir, 1973). Figure (15) shows the RMS error graph for different weights used in this study that successfully converged to pre-set tolerant value.

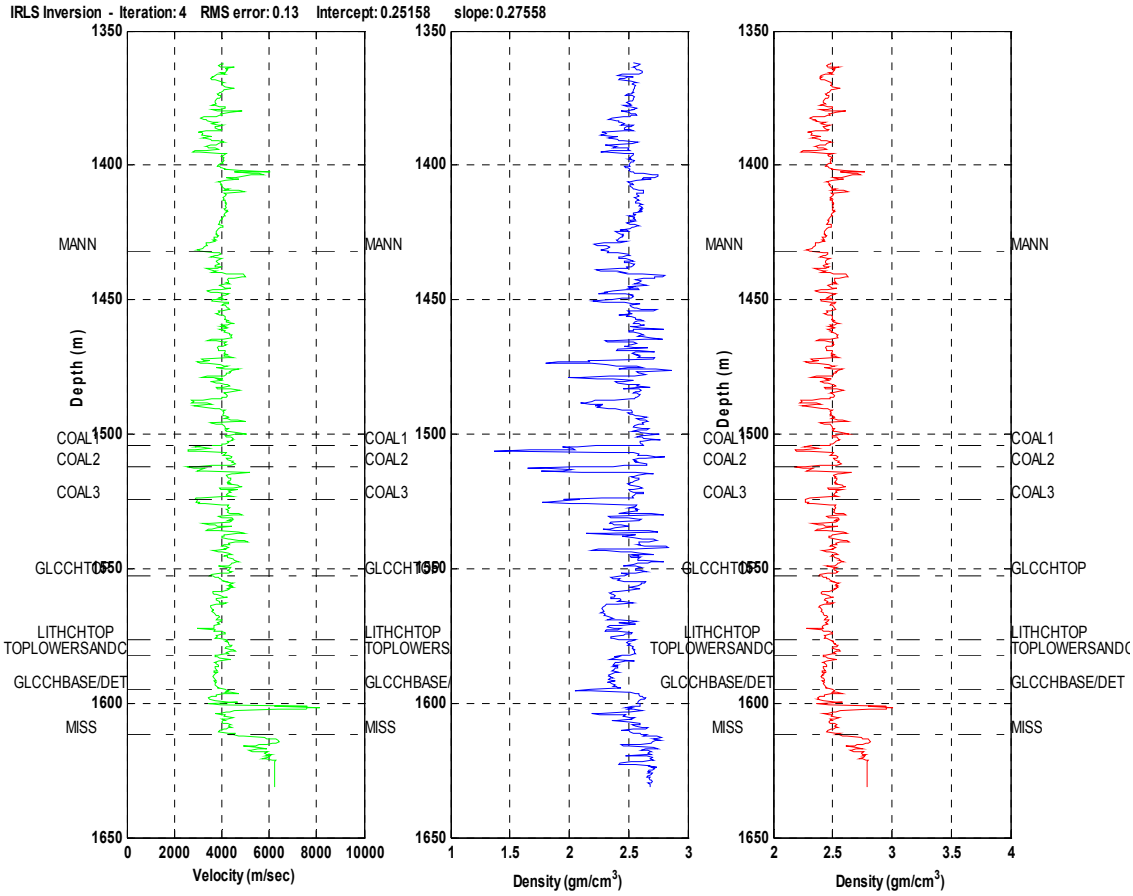

FIG.11. Well 08-08: IRLS inversion of density log using AM- weight function.

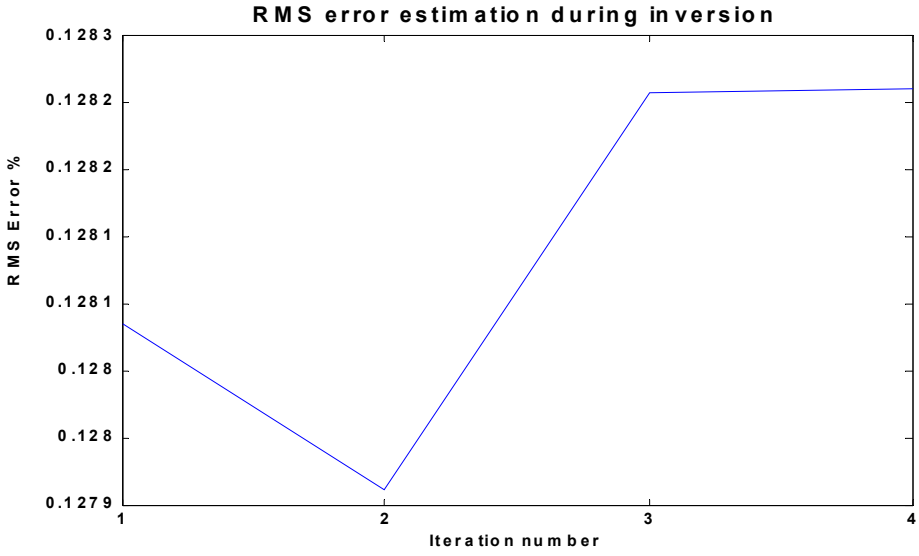

FIG.12. Well 08-08: RMS error during IRLS inversion using AM- weight function.

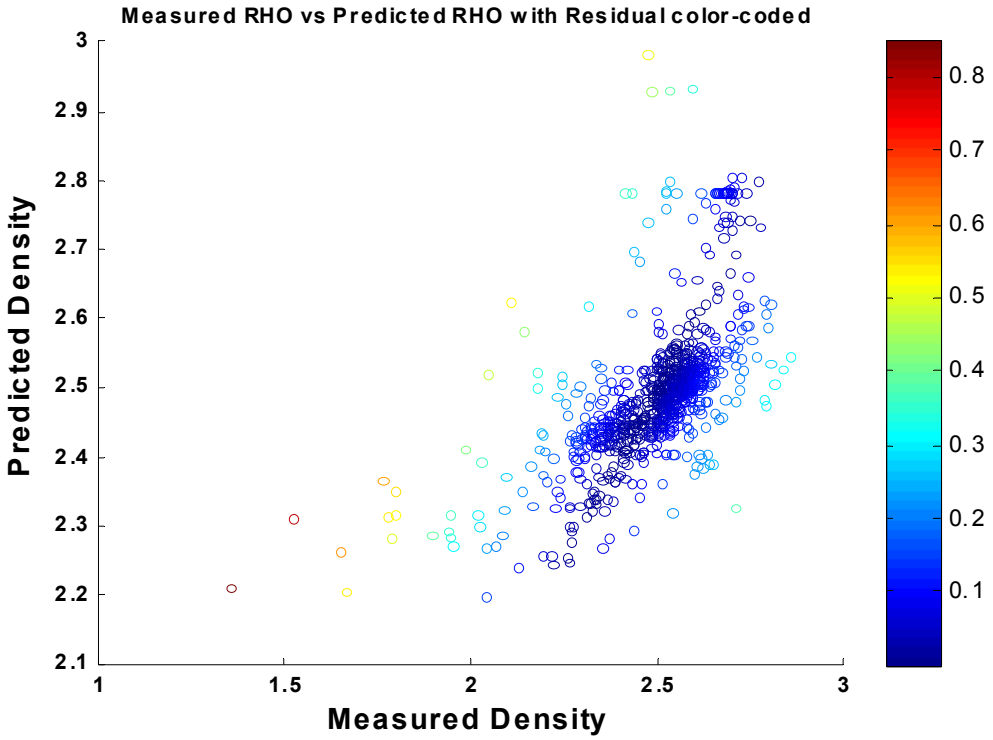

FIG.13. Well 08-08: Measured versus predicted density log with residual color-code. Constrains applied in data-space.

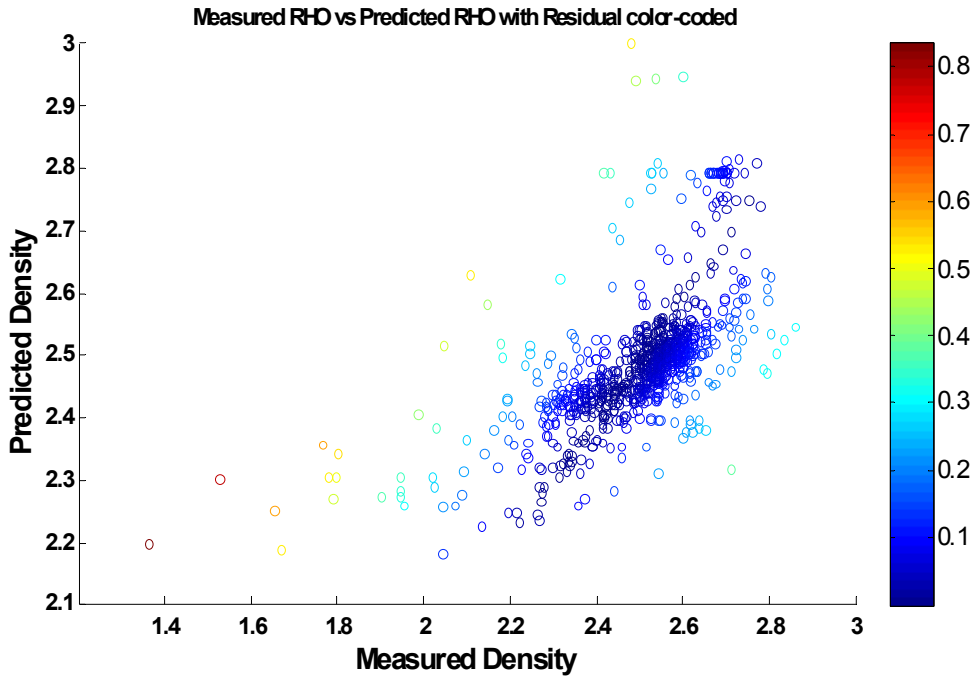

FIG.14. Well 08-08: Measured versus predicted density log with residual color-code. Constrains applied in model-space.

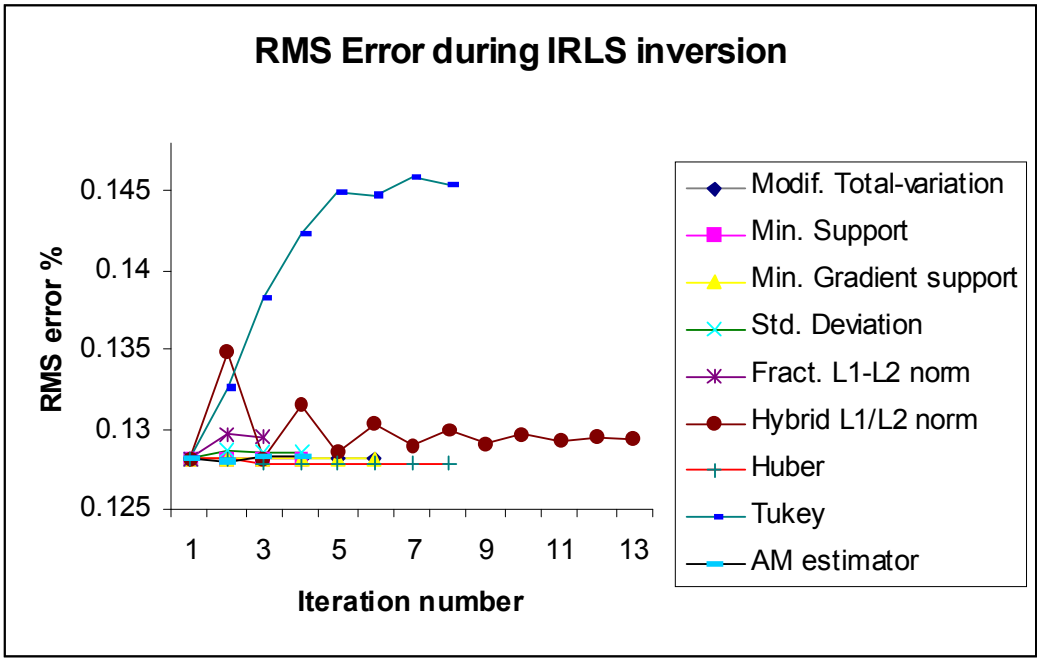

FIG.15. Well 08-08: RMS Error during IRLS inversion using different weight functions.

Improving the signal to noise ratio by focusing predicted data is one of many advantages of inverse problem. In figure (16), the measured density (left panel) and inverted density (right panel) are plotted against Vp/Vs. Two major regions of densities can be recognized in the predicted density panel. The first region that represents the sandstone has density in the range of 2.5 -2.8 gm/cm^3, while the second region that would represent carbonate rock, has density range of ≤ 2.8 gm/cm^3.

IRLS INVERSION OF NOISY DATA LOG

Cycle skipping is a serious problem in density well logging. Those outliers mask good portion of the log if not manipulated. Frequent repeating of cycle skipping could also result from equipment malfunctions that produce erroneous density values. These abnormal values are highly inconsistent with other density values, making the density log less interpretive. Such problem can be overcome by utilizing robust inversion (Claerbout and Muir, 1973) algorithm, which is less sensitive to these outliers when proper weight constrains are incorporated in the inverse problem.

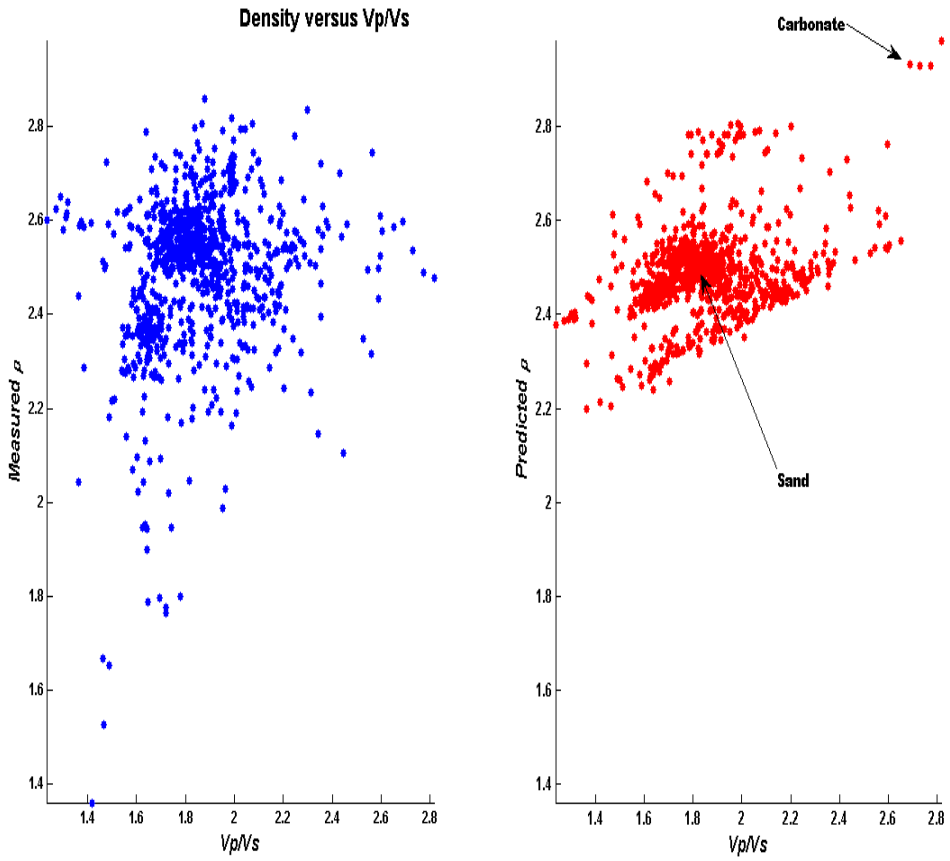

FIG.16. Observed and inverted density versus Vp/Vs.

Since the inverse algorithm used in this study relies mainly only the sonic P-wave velocity, V_P, in generating synthetic density data, random noise of magnitude of 5% with zero mean and variance not equal to 1 were added to the sonic log. The Huber weight method is used during the inversion of this noisy data.

Figure (17) shows the inverted log of noisy data, while figure (18) shows the RMS error. The inverted density log still shows major events that are corresponding to lithology change are mapped well, but with less resolution compared to the noise-free data showed earlier in figure (9).

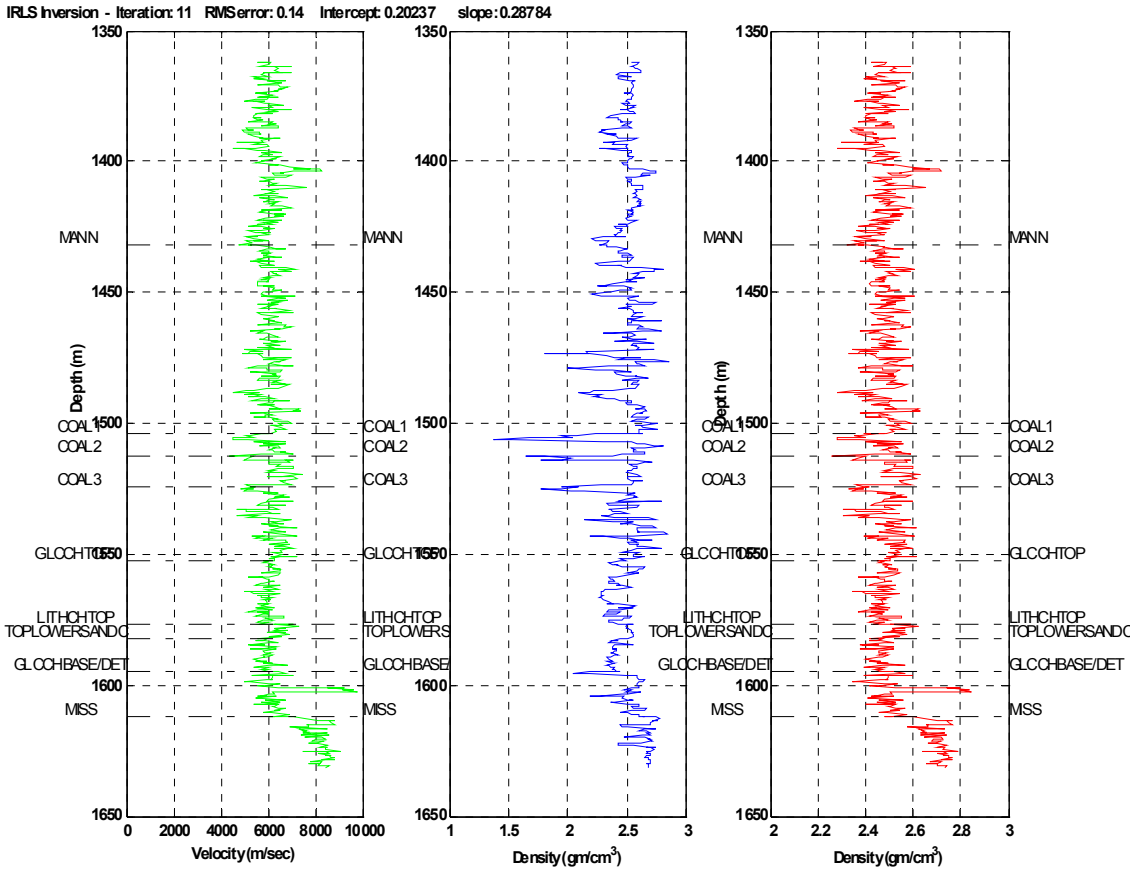

FIG.17. Well 08-08: IRLS inversion of noisy density log using AM- weight function.

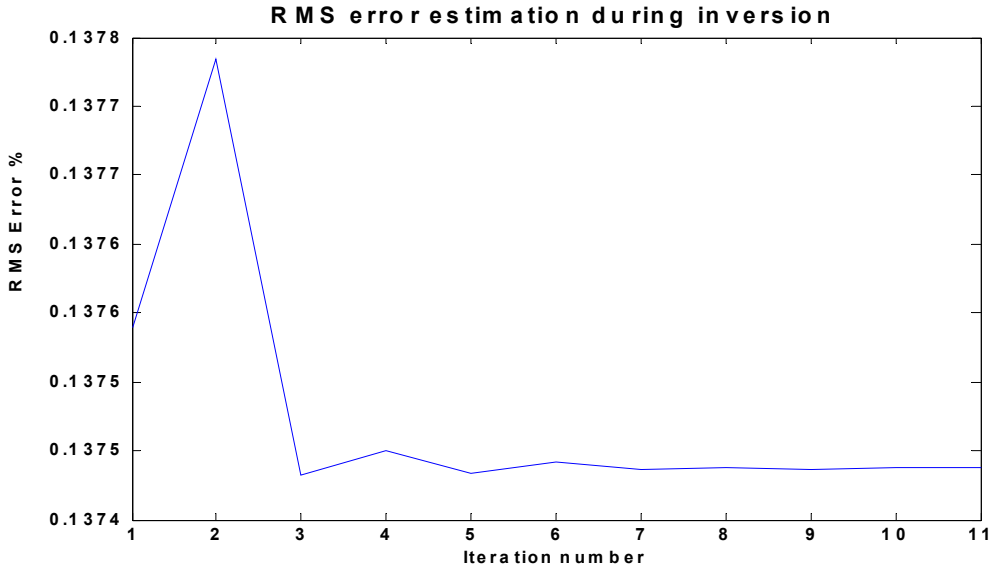

FIG.18. Well 08-08: RMS error during IRLS inversion of noisy data using Huber weight function.

PREDICTED DENSITY LOG FROM JOINT-INVERSION OF V_P & V_S LOGS

Russell et al., (2004) used multi-regression method so as to improve the mud-rock line estimation. The regression method was done separately for each log and estimated attribute were compiled to predict sonic shear log.

In this study, joint inversion of sonic Vp and Vs logs were done simultaneously to predict density log. In order to accomplish this inverse scheme, equation (1) has been modified to have two different operators, where estimated residuals from each log can be applied independently, and also to have different damping factor applied to each log. The model regularization operator was set to be firs-order difference operator. The joint-inverse equation is written as

$$\left[(G_1^T W_{d_1}^T W_{d_1} G_1 + \lambda_1 W_m^T W_m) + (G_2^T W_{d_2}^T W_{d_2} G_2 + \lambda_2 W_m^T W_m)\right] m = \left[(G_1^T W_{d_1}^T W_{d_1} d) + (G_2^T W_{d_2}^T W_{d_2} d)\right] \quad (15)$$

Figure (19) shows the inversion of density log using joint-inversion equation (15). The predict model for each log as well as total logs were plotted together. The predict density log using Vp and total logs show very good resemblances. However, there is a shift-gap between measured density and predict density when using Vs log calculating predict density log. This can be attributed to the different physical properties that were used in inverse operators, knowing that Vp magnitude is almost double Vs values. Figure (20), displays predicted density using Vp log and total logs, while figure (21) shows RMS error of individual log as well as for total logs. The final model converged within 2 iterations.

CONCLUSIONS

Regardless of noise level, the re-weighted inverse algorithm of density log shows fast convergence to a lowest *RMS-error* value within few numbers of iterations. The weighted constrain functions imposed in the data-space produce blocky sections with small residual magnitude compared to constrain added in model-space. The *RMS* error curve shows some improvements, as algorithm converges towards final model. The sand baseline can be easily recognized from inverted density log. The scatter display of inverted density log versus Vp/Vs log can aid in lithology discrimination. The joint inversion of multi logs further improves the predicted density log.

ACKNOWLEDGEMENTS

Thanks to Dr. Brian Russell of Hampson-Russell Co., for constructive suggestions to this study, and all of the CREWES sponsors.

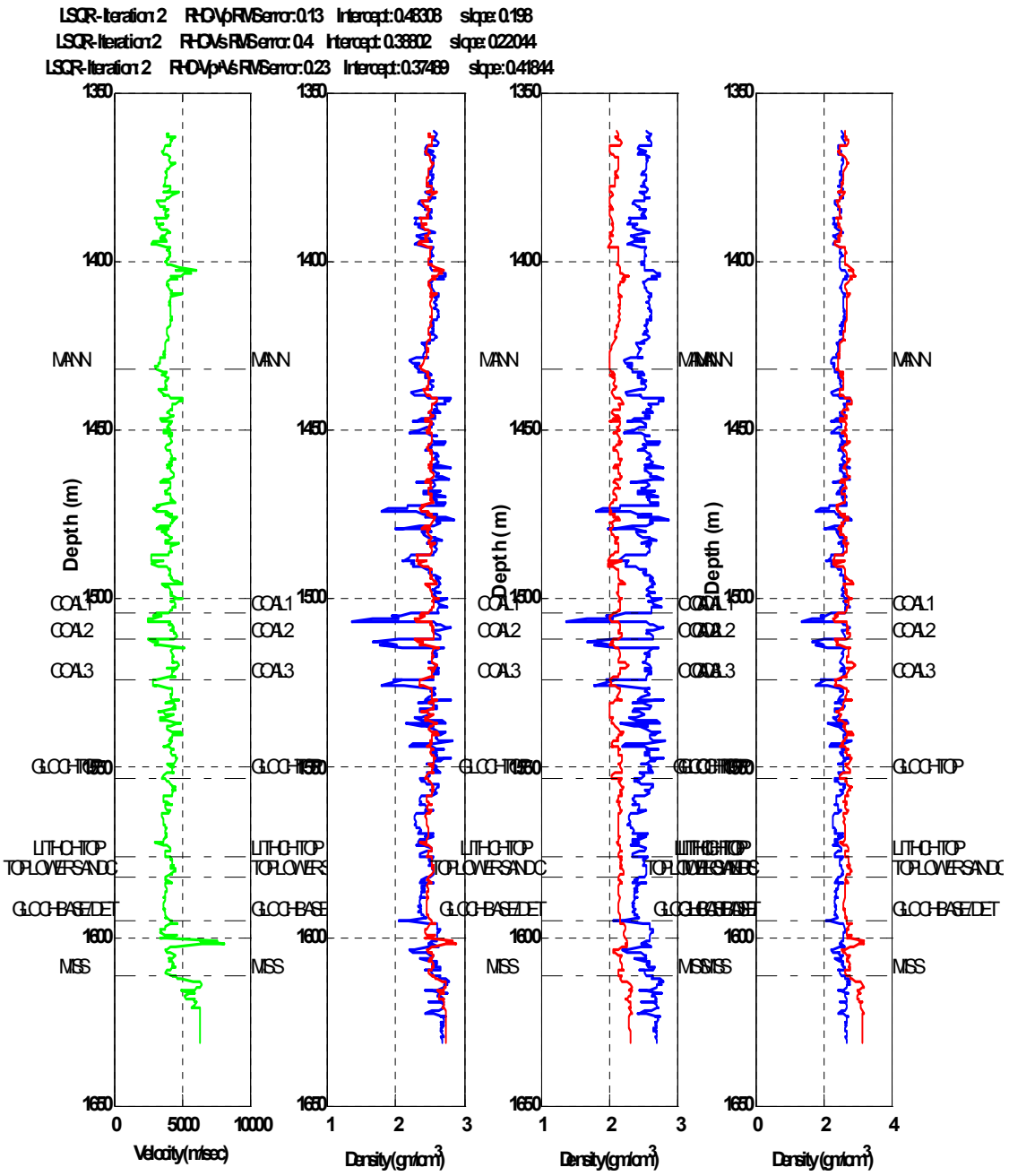

FIG.19 Well 08-08: IRLS joint inversion of Vp & Vs to predict density log using Huber weight.

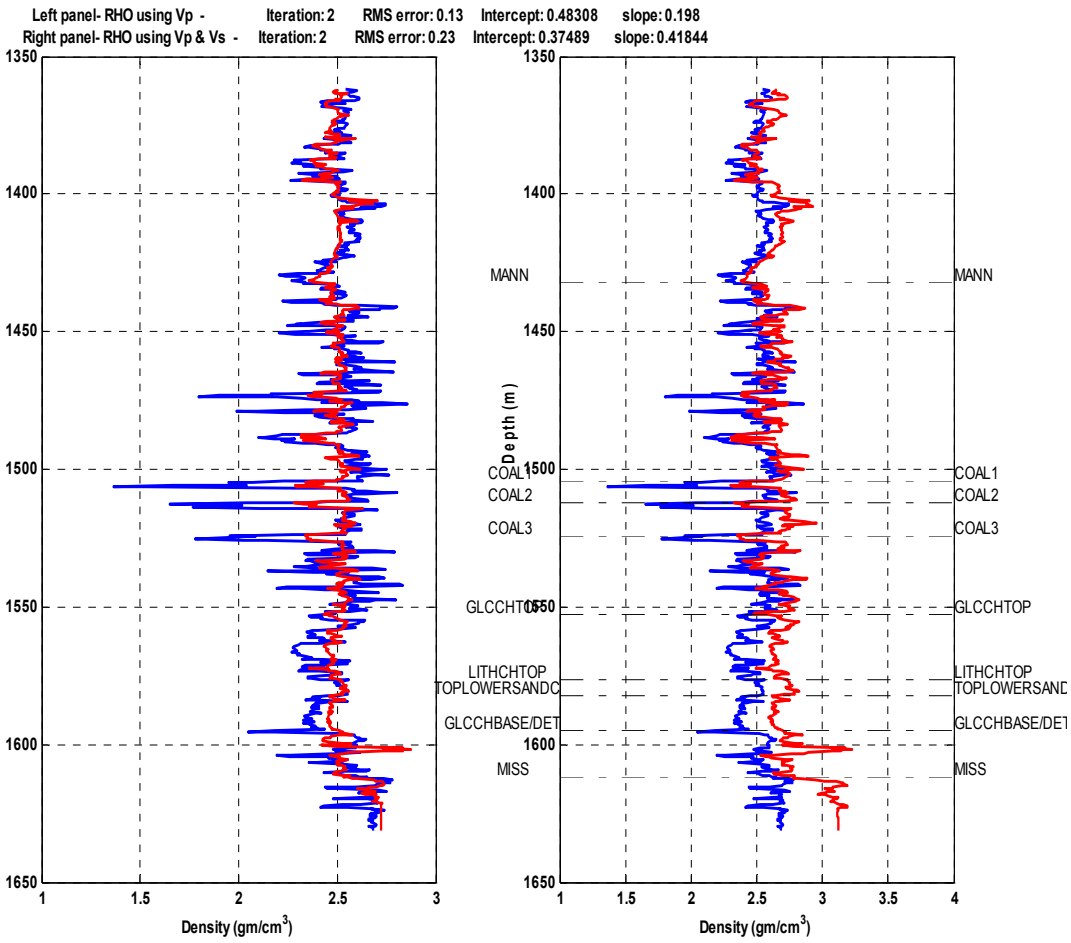

FIG.20. Well 08-08: IRLS joint inversion of Vp & Vs to predict density log.

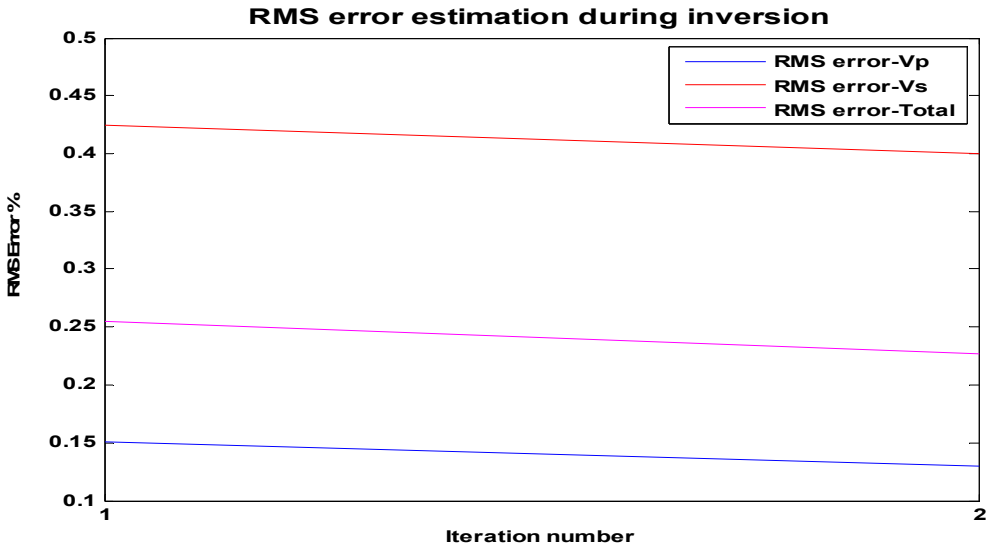

FIG.21.Well 08-08: RMS error during IRLS joint inversion of Vp & Vs to predict density log.

REFERENCES

Aster, R.C., Borchers, B. and Thurber, C.H., 2005, Parameters estimation and inverse problem : Elsevier Academic Press.

Bube, K.P., and Langan, R.T., 1997, Hybrid lambda1/lambda2 minimization with application to tomography: Geophysics, **62**, 1183-1195.

Claerbout, J.F. and Muir, F., 1973, Robust modeling with erratic data: Geophysics, **38**, 826-844.

Darche, G., 1989, Iterative l1 deconvolution: SEP-Report, **61**, 281-301.

Holland, P. W., and Welsch, R. E., 1977, Robust regression using iteratively reweighted least squares: Comm. Statist., **A6**, 813-827.

Hong, X., and Chen, S., 2005, M-estimator and D-optimality model construction using orthogonal forward regression: IEEE Transaction on systems, Man, and Cybernetics- Part B, Cybernetics*, **35**, 155-162.*

Huber, P. J., 1981, Robust statistics: J. Wiley, New York Publisher.

Li, S.Z., 1996, Robustizing robust M-estimation using deterministic annealing: Pattern Recognition, **29**, 159-166.

Rücker, C. & Günther, T.,2006, A general approach for introducing structural information - From constraints to joint inversion: EAGE Near Surface Geophysics Meeting.

Russell, B.H., Lines, L.R., and Hampson, D.P., 2004, A case study in the local estimation of shear-wave logs: CREWES report, **16**, 1-7

Varga, R.S., 1962. Matrix iterative analysis: Prentice Hill Publisher.

Wolke, R., and Schwetlick, H., 1988, iteratively re-weighted least squares algorithms, convergence analysis, and numerical comparisons: SIAM Journal of Scientific and statistical computation, **9**, 907-921.